

Network Traffic Reduction in Six Degree-of-Freedom Haptic Telementoring Systems

¹Nizar Sakr, ¹Jilin Zhou, ^{1†}Nicolas D. Georganas, ²Jiying Zhao, and ¹Emil M. Petriu

Distributed and Collaborative Virtual Environments Research Laboratory (DISCOVER),

School of Information Technology and Engineering (SITE), University of Ottawa,

800 King Edward Ave., Ottawa, ON, Canada, K1N 6N5

Phone: (613) 562-5800 ext. 2148, Fax: (613) 562-5175

¹{nsakr, jzhou, georganas, petriu}@discover.uottawa.ca, ²{jyzhao}@site.uottawa.ca

Abstract— This paper introduces a haptic data reduction and transmission technique to reduce the packet rate in six Degree-of-Freedom (6-DoF) haptic-enabled telementoring systems. The presented method relies on the limitations of human haptic perception (i.e. the Just Noticeable Differences) with respect to a user's hand position and orientation in order to reduce the number of packets transmitted without compromising transparency. A haptic prediction model is exploited to further reduce the amount of haptic packets transmitted, and to improve the reconstruction of data samples on the receiver side. Several distance metrics are also discussed to evaluate the acuity of human haptic perception when data reduction is performed in 6-DoF settings. Psychophysical experiments validate the effectiveness of the suggested algorithm as great haptic data reduction is achieved (up to 96%), while preserving the overall quality of the telementoring environment.

I. INTRODUCTION

Haptic telementoring can be generally defined as remote mentoring via a communication network, while incorporating the sense of touch. Its applications in tele-education are numerous. In particular, it has garnered significant interest in recent years in tele-surgical training. This is primarily due to the fact that procedures in medical applications are not easily illustrated using solely audio and visual cues. For example, haptic guidance permits a novice surgeon to perform laparoscopic procedures with the assistance of a remote expert via telementoring [1]. This is of particular importance since expert surgeons are generally primarily concentrated in major cities, and are therefore often not readily available at remote locations especially near battlefield sites.

Practically, a haptic-enabled telementoring scenario encompasses a mentor and a mentee linked over a packet switched communication network (e.g. the Internet), where each is equipped with a haptic device as well as an audio-visual interface. Moreover, telementoring can be regarded as a branch of bilateral telehaptics (i.e. networked haptics), it however differs from conventional teleoperation systems in its flexible control architecture that can adapt to different learning scenarios and modalities. In haptic telementoring systems velocity, orientation and position data packets are exchanged between the mentor and the student. Moreover,

[†]N.D. Georganas holds a Cátedra de Excelencia at the Univ. Carlos III de Madrid and is visiting researcher at IMDEA Networks, on leave from the School of Information Technology and Engineering, University of Ottawa.

the local control loops at the mentor and student sites operate in the range of 500-1000 Hz. In order to limit packetization and transmission delays which could greatly compromise the stability of the system, every set of sampled data is typically transmitted in individual packets. However, high packet rates, which in this case are in the range of 500-1000 packets per second, are difficult to sustain over long distance digital communication networks.

In [2], [3], Hinterseer *et al.* introduced a perception-based haptic data reduction where haptic data are only transmitted if the difference between the current and the most recently transmitted sample exceeds a predefined human-perception threshold. This work is extended in [4], where a prediction based on linear extrapolation is discussed in order to further reduce the amount of haptic data packets sent over a network. Their technique is demonstrated to work well in 1-DoF and 3-DoF telepresence systems. However, teleoperation systems that rely on only 1-DoF or 3-DoF haptic devices impose a great restriction on the operator, since manipulation inherently requires six degrees of freedom. Consequently, 6-DoF devices provide the user with a more realistic haptic experience, as full force and torque feedback is available. However an increase of the number of DoFs, from 3-DoF to 6-DoF evidently renders perceptual haptic data reduction a more challenging problem.

In this paper, a haptic data reduction and transmission technique is introduced to reduce the packet rate in 6-DoF telehaptic systems, while taking into account the bilateral and flexible nature of telementoring environments. The presented method relies on the limitations of human haptic perception (i.e. the Just Noticeable Differences) with respect to a user's hand position and orientation in order to reduce the number of packets transmitted without compromising transparency. Also, distance metrics are derived and included in the algorithm, to ensure that distortions introduced by the data reduction technique never exceed the human haptic perception threshold.

The rest of the paper is organized as follows. In Section II, haptic-enabled telementoring using 6-DoF devices is illustrated. In Section III, the proposed haptic data reduction and transmission technique is presented. In Section IV, the materials and methods used during the experimental procedure are illustrated. In Section V, the experimental

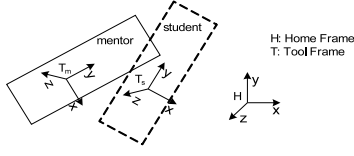


Fig. 1. 6-DOF Telementoring Diagram

results are provided. Finally, conclusive remarks are outlined in Section VI.

II. HAPTIC-ENABLED TELEMENTORING

With 6-DOF haptic-enabled telementoring, the student not only feels the spatial trajectory movements of the mentor but also the dynamic handling of the virtual tool in terms of rotational trajectory. We describe them together as kinematic trajectories. The force/torque values sent to the haptic device at the mentor site (S_m) and the student site (S_s) are accordingly separated into two parts: translational force $F = [f_x \ f_y \ f_z]^T$ which brings the origins of the two tool frames together and rotational torque $\tau = [\tau_x \ \tau_y \ \tau_z]^T$ which aligns the axes of the two tool frames as shown in Fig. 1. The final joint torque τ_{motor} sent to each motor is computed as

$$\tau_{motor} = J^T \begin{bmatrix} F \\ \tau \end{bmatrix}, \quad (1)$$

where J is the Jacobian matrix of the device at the current configuration.

The force values are depicted below in Equ. (2) and Equ. (3) respectively.

$$\begin{aligned} F_m &= F_{mc} + F_{me}, \\ &= K_{mp}(x_{cs} - x_m) + K_{md}(\dot{x}_{cs} - \dot{x}_m) + F_{me}. \end{aligned} \quad (2)$$

$$\begin{aligned} F_s &= F_{sc} + F_{se}, \\ &= K_{sp}(x_{cm} - x_s) + K_{sd}(\dot{x}_{cm} - \dot{x}_s) + F_{se}. \end{aligned} \quad (3)$$

The first two terms in (2) and (3) form the expression of a classical proportional-derivative controller, where K_{mp} and K_{sp} denote the adjustable proportional gains at S_m and S_s , whereas K_{md} and K_{sd} correspond to the derivative gains. Practically, the mentor can adjust K_{sp} based on the student's performance or the current network latency. If the student is confident of his or her skills, the mentor (or the student for that matter) can lower the value of K_{sp} to enable the trainee to feel more force feedback from the simulation itself. On the other hand, if the network latency is too large, both sites should decrease this proportional gain to improve the stability margin of the closed-loop system.

There are several methods to represent rotations in three dimensions. The three most popular representations are: 3×3 rotational matrix, Euler angles, and Quaternion. Quaternion is chosen here for its direct relationship with torque and for its computational simplicity, e.g. the inverse operation

is easily achieved. Given a rotation matrix R , the associated unit quaternion is defined as

$$Q = (q_0, \vec{q}) = (\cos(\theta/2), \omega \sin(\theta/2)), \quad (4)$$

where q_0 is the scalar component of Q , $\vec{q} = \{q_1, q_2, q_3\}$ is the vector component, $\omega \in \mathbb{R}^3$ represents the unit axis of rotation and $\theta \in \mathbb{R}$ represents the angle of rotation [5]. Let Q_m and Q_s denote the rotation of the tool frame T_m and T_s with respect to the home frame. The rotation between T_m and T_s is then

$$Q_{ms} = Q_m \cdot Q_s^{-1}. \quad (5)$$

The torque values are then depicted below in Equ. (6) and Equ. (7) respectively.

$$\begin{aligned} \tau &= \tau_{mc} + \tau_{me}, \\ &= K_{mTorque}(Q_{\vec{q},cs} \cdot Q_{\vec{q},m}^{-1}) + \tau_{me}. \end{aligned} \quad (6)$$

$$\begin{aligned} \tau &= \tau_{sc} + \tau_{se}, \\ &= K_{sTorque}(Q_{\vec{q},cm} \cdot Q_{\vec{q},s}^{-1}) + \tau_{se}. \end{aligned} \quad (7)$$

The first term in (6) and (7) is used to diminish the value of θ_{ms} such that the two tool frames are aligned. Because $\vec{q} = \omega \sin(\theta/2)$, the magnitude of this alignment torque will be capped at K_{torque} when $\theta = \pm\pi$. In addition, the sign $q_0 = \cos(\theta/2)$ should be carefully tracked as a sign change indicates a flip of the rotation axis ω . To avoid the induced jumps of the alignment torque, the rotation axis ω is always flipped in case of negative q_0 . The algorithm to calculate this alignment torque is given as follows:

$$\begin{aligned} Q_{ab} &= Q_a \cdot Q_b^{-1} \\ \text{if } (Q_{q_0,ab} < 0) \text{ then } Q_{\vec{q},ab} &= -Q_{\vec{q},ab} \\ \tau_{ab} &= K_{torque} * Q_{\vec{q},ab} \end{aligned}$$

III. HAPTIC DATA REDUCTION AND TRANSMISSION

In this section, a haptic data reduction and transmission method to reduce the number of transmitted packets in 6-DoF haptic-enabled telementoring systems is presented.

A. Haptic Perceptibility

The suggested transmission technique exploits the limitations of human haptic perception in order to reduce the amount of data packets sent over a packet switched network. Human haptic perception is generally analyzed using the concept of Just Noticeable Differences (JND). The JND consists of the minimum amount of change in stimulus intensity which results in a noticeable variation in sensory experience. Numerous psychophysical studies have been conducted in the literature to derive the JND of haptic perception. For kinesthetic force feedback (typically exploited in haptic telementoring systems), several factors impact the overall human haptic perception JND, including force, pressure, velocity, as well as the position of the joints. Generally, the JND for human haptic perception is in the range of 5% to 15%

[6], [7]. This suggests that, in a telementoring system, if the change in magnitude of the haptic force currently applied by the mentor is less than the JND, the mentee would not perceive a force-feedback variation. This concept is used in the suggested packet reduction method, where haptic data are only transmitted if the remote operator is likely to perceive a change in the kinesthetic force-feedback response.

B. Deadband Principle

The deadband principle essentially states that signal changes do not need to be transmitted over the communication network unless they exceed a fixed or a magnitude-dependent threshold [4], [8]. The presented method however relies on the limitations of human haptic perception with respect to a user's hand position and orientation in order to reduce the number of packets transmitted. Consequently, to determine whether it is necessary to transmit newly acquired data samples, a perceptual distance metric must be defined that considers both, hand position and orientation information. A possible formulation of this problem can be depicted using the deadband principle as follows:

if ($D_p(\mathbf{p}_i, \mathbf{p}_c) > f(\mathbf{p}_i)$ or $D_o(\mathbf{o}_i, \mathbf{o}_c) > f(\mathbf{o}_i)$)
then transmit $\mathbf{p}_c, \mathbf{o}_c$
else do not transmit

where \mathbf{p}_i and \mathbf{p}_c denote the initial and the currently acquired position vectors, whereas \mathbf{o}_i and \mathbf{o}_c correspond to the initial and the currently acquired orientation vectors. $D_p(\cdot)$ and $D_o(\cdot)$ consist of distance metrics used to measure the proximity between position and orientation vectors respectively. $f(\mathbf{p}_i)$ and $f(\mathbf{o}_i)$ define the perceptual thresholds, i.e. the region (referred to as the deadzone) in which transparency is maintained. Therefore, in order to determine whether to transmit the currently acquired data vectors \mathbf{p}_c and \mathbf{o}_c , the distance between \mathbf{p}_c and the initial position vector \mathbf{p}_i , and the distance in orientation between \mathbf{o}_c and \mathbf{o}_i must be larger than $f(\mathbf{p}_i)$ and $f(\mathbf{o}_i)$ respectively. Furthermore, the method relies on a fixed position deadband d_p and a fixed orientation deadband d_o with deadzones of radius $f(\mathbf{m}) = d_m$, where $\mathbf{m} \in \{\mathbf{p}, \mathbf{o}\}$.

1) *Position Distance Metric*: In order to measure the proximity of two position vectors \mathbf{p}_i and \mathbf{p}_c , the Euclidean distance is computed, as follows:

$$D_p(\mathbf{p}_i, \mathbf{p}_c) = |\mathbf{p}_i - \mathbf{p}_c| = \sqrt{(\mathbf{p}_{i,x} - \mathbf{p}_{c,x})^2 + (\mathbf{p}_{i,y} - \mathbf{p}_{c,y})^2 + (\mathbf{p}_{i,z} - \mathbf{p}_{c,z})^2}. \quad (8)$$

2) *Orientation Distance Metric*: The convention used when representing and parameterizing rotations in three dimensions must be considered when defining a distance metric to express the similarity (or "closeness") between two different orientations. The following two common representations will be discussed: Euler angles and unit quaternions. First, according to Euler's rotation theorem, any orientation can be illustrated by a sequence of three rotations (α, β, γ)

about a set of three axes (x_1, x_2, x_3) . Considering that the common roll-pitch-yaw euler angles convention is used, the angular distance between two orientations $\mathbf{o}_i = (\alpha_i, \beta_i, \gamma_i)$ and $\mathbf{o}_c = (\alpha_c, \beta_c, \gamma_c)$ can be computed as follows:

$$D_o(\mathbf{o}_i, \mathbf{o}_c) = \sqrt{S(\alpha_{i,x}, \alpha_{c,x})^2 + S(\beta_{i,y}, \beta_{c,y})^2 + S(\gamma_{i,z}, \gamma_{c,z})^2}. \quad (9)$$

The $S(\cdot)$ function is defined to ensure that the "shortest path" difference between two angles is considered, as follows:

$$S(\theta_1, \theta_2) = \begin{cases} \Delta\theta + 2\pi & \text{if } \Delta\theta < -\pi \\ \Delta\theta - 2\pi & \text{if } \Delta\theta > \pi \\ \Delta\theta & \text{otherwise} \end{cases} \quad (10)$$

where $\Delta\theta = \theta_2 - \theta_1$ and $\Delta\theta \in [-\pi, +\pi]$. An important advantage of euler angles is their intuitive physical interpretation. However, a drawback of this representation is that its parametrization is not unique, i.e. there are multiple sets of parameter values which can result in the same rotation [9]. This limitation makes euler angles less attractive when used to measure the proximity of two orientations as it might in certain cases overestimate the distances. An alternative metric to measure rotation distances can be defined using the unit quaternion representation. Given two unit quaternions $Q_i = \{q_{0,i}, q_{1,i}, q_{2,i}, q_{3,i}\}$, and $Q_c = \{q_{0,c}, q_{1,c}, q_{2,c}, q_{3,c}\}$, (where in this case, $\mathbf{o}_i \Leftrightarrow Q_i$, and $\mathbf{o}_c \Leftrightarrow Q_c$) the difference in rotation can be computed as follows:

$$D_o(Q_i, Q_c) = 2 * \arccos(|Q_i \cdot Q_c|), \quad (11)$$

where the inner product between the two quaternions is defined as follows:

$$Q_i \cdot Q_c = q_{0,i}q_{0,c} + q_{1,i}q_{1,c} + q_{2,i}q_{2,c} + q_{3,i}q_{3,c} \quad (12)$$

Another approach to measuring the difference in orientation using unit quaternions, is to simply compute the absolute inner product between the two vectors. In this case, computed distances are in the range $[0,1]$, where small rotation differences result in distances that are closer to 1.

C. Haptic Prediction Model

A haptic prediction model is derived in order reduce the amount of haptic packets transmitted, and to improve the reconstruction of missing data samples. It encompasses three different module: a least-square estimator, a median filter as well as a linear predictor. This model is used to predict both, position and orientation information. Furthermore, in this phase of the data reduction algorithm, orientation is represented using euler angles as it is more intuitive and convenient to predict angles as opposed to unit vectors (quaternions). This being said, haptic data prediction is computed as follows¹:

$$\begin{aligned} \hat{g}(n+1) &= \hat{g}(n)\Delta T + g(n) \\ &= \hat{v}(n)\Delta T + g(n), \end{aligned} \quad (13)$$

¹The prediction model is illustrated for one dimensional signals; its extension to multidimensional data is however straightforward.

IV. MATERIALS AND METHODS

A. Experimental Setup

The experimental setup consists of two identical haptic devices connected to two separate PCs over a 100 Mbps Ethernet local area network. The haptic stimuli at both, the mentor end and the mentee (i.e. student) end are refreshed at a rate of 1000 Hz. Essentially, packets between the two PCs are transmitted at a rate of 1 kHz. The suggested haptic data reduction and transmission technique is executed on both PCs due to the bilateral nature of telementoring systems. Consequently, haptic data are bilaterally transmitted between the mentor PC and the mentee PC. This is necessary in order to allow for the direct coupling of the haptic devices over the communication network, and in turn, enable a hand-by-hand teaching experience. The force values sent to the haptic device motors at S_m and S_s are as depicted in Section II. The experiments were conducted using MPB's high fidelity Freedom 6S haptic devices, which provide haptic force feedback in 6 degrees of freedom.

B. Subjects

Altogether, 8 subjects (5 males and 3 females, aged 25-35), 7 right handed and 1 left handed with no known sensorimotor impairments with their hands took part in the experiments. Their prior experience with force-feedback haptic devices ranged from novice to expert.

C. Procedure

The experiments were arranged in three blocks per subject: a practice block and two experimental blocks. Moreover, the practice and the experimental blocks follow the same procedure, however, the practice block is intended to familiarize the subjects with the haptic telementoring system and to give them a feel of the distortion encountered when the suggested haptic packet reduction technique is enabled. Each block consisted of a number of runs that differ in the position and orientation deadband size. Twelve different position deadband (d_p) values were used and are as follows: 0 mm, 0.05 mm, 0.1 mm, 0.2 mm, 0.3 mm, 0.4 mm, 0.5 mm, 0.7 mm, 0.9 mm, 1.1 mm, 1.5 mm, and 2.0 mm. Similarly, eleven different orientation deadband values were exploited and they consist of: 0.0 rad, 0.0005 rad, 0.001 rad, 0.002 rad, 0.003 rad, 0.004 rad, 0.005 rad, 0.006 rad, 0.008 rad, 0.01 rad, and 0.012 rad. Therefore, in total $12 \times 11 = 132$ different runs per block were performed using different randomly selected combinations of deadband values. After every run the subjects were requested to rate the haptic telementoring experience using the following five-grade impairment scale:

- 5 – Imperceptible
- 4 – Perceptible, but not annoying
- 3 – Slightly annoying
- 2 – Annoying
- 1 – Very annoying

Users were also permitted to give in-between values when necessary (i.e. 4.5, 3.5, 2.5, and 1.5) to better assess their

where $g(n)$ denotes the current position/euler angle values, $\hat{v}(n)$ is the current estimated movement velocity/euler angle rate-of-change, $\hat{g}(n+1)$ corresponds to the predicted position/angle estimate, whereas ΔT is the sampling period. In turn, the transmission method exploits the suggested linear prediction technique as follows:

$$g_i = \begin{cases} g_{new} & \text{if packet sent or received} \\ g_{i-1} + \hat{v}_{new} \cdot \Delta T & \text{otherwise} \end{cases}$$

where g_{new} and \hat{v}_{new} are the newly transmitted or received position/angle and velocity/angle-rate-of-change data samples respectively, g_i and g_{i-1} are the most recent outputs of the prediction model, whereas ΔT is the sampling period. Essentially, when the predictor is used on the transmitting end, the predicted value must fall within the predefined deadzone (defined by the deadband $d_m \in \{d_p, d_o\}$), otherwise a new sample is transmitted over the network. Conversely, when the predictor is exploited on the receiving end of the data reduction techniques, it attempts to reconstruct the missing haptic data samples based on previously received packets. Hence, the prediction model compensates for missing data packets or introduced communication delay to regularly provide the haptic-real time controller (used to calculate forces to send to the haptic device) with data samples at a consistent rate of 1 kHz or better. This is necessary in order to guarantee the stability of the closed-control loops, and in turn maintain compelling and stable force feedback at the mentor site (S_m) and the mentee site (S_s).

It can be observed from (13), that the prediction performance can be positively or negatively affected depending on the precision of the acquired position (or orientation) and velocity (or angle-rate-of-change) data. Generally, the noise present in position and orientation readings is low due to the fact that haptic devices are typically equipped with joint sensors. However, velocity (whether movement velocity, or euler angles' rate-of-change) is generally derived using the finite difference method which leads to very noisy velocity estimates at high sampling frequencies [10]. This being said, in order to obtain more precise estimates, linear (FIR) filtering is performed as follows:

$$\hat{v}(n) = \sum_{i=0}^{M-1} w(i)g(n-i), \quad (14)$$

where $w(i)$ corresponds to the filter coefficients whereas M denotes the filter length. Essentially, a velocity estimate $\hat{v}(n)$ (i.e. the slope) that would best fit the observation data $g(n)$ in the least-square sense is derived. Moreover, the corresponding filter coefficients can be computed using the standard least-square method as follows:

$$w(i) = \frac{12 \left(\frac{M-1}{2} - i \right)}{T_s M (M^2 - 1)}, \quad 0 \leq i \leq M-1 \quad (15)$$

Furthermore, median filtering is also used to eliminate any fine irregularities and outliers remaining in the computed velocity/angle-rate-of-change measures, while preserving the true signal discontinuities [11].

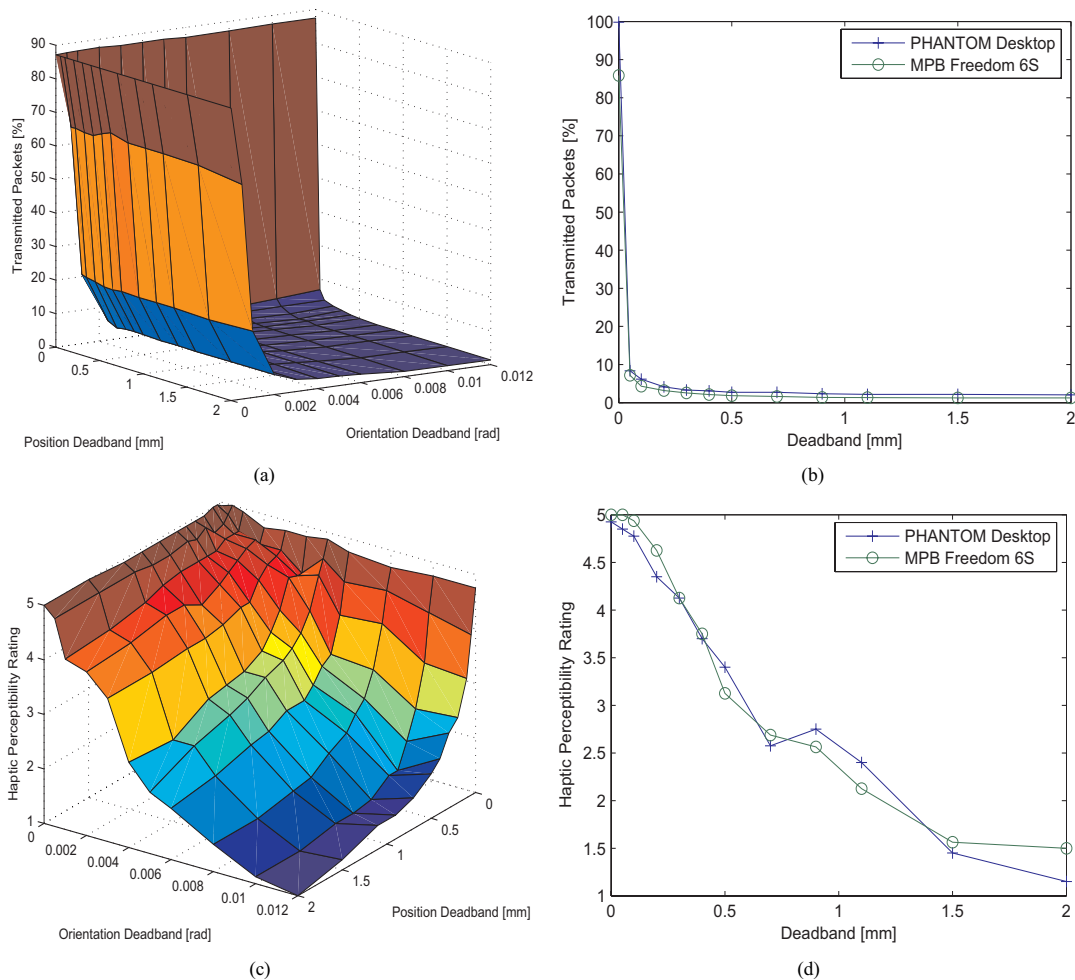


Fig. 2. Results of the haptic packet reduction technique in (a), (c) 6-DoF and (b), (d) 3-DoF haptic telementoring systems.

opinion. Furthermore, in order to demonstrate the scalability of the suggested multi-DoFs haptic data reduction algorithm, another experiment was performed, however in this case, torque feedback was deactivated. In other words, orientation information was not considered, and only 3-DoF force feedback was provided (only the position deadband values were used). For the sake of comparison across different haptic devices, this latter experiment was repeated while replacing the Freedom 6S devices with two high-precision Sensable PHANTOM Desktop devices. These experiments are intended to demonstrate that the algorithm scales well when extending a 3-DoF haptic telementoring system to 6-DoFs.

V. EXPERIMENTAL VERIFICATIONS

In this section, an evaluation of the haptic data reduction technique is performed. The displaying stimuli of the experiment are initially presented, followed by a concise description of the experimental results.

1) *Displaying Stimuli*: A simple experimental environment is used to enable an unbiased validation of the suggested method. Essentially, during each run, users are requested to trace a periodic sinusoidal signal (of period equal to 5 cm and peak-to-peak amplitude of 15.5 cm) for a duration of approximately 20 seconds. The participant acts as the mentor and repeatedly traces a sketch of the sinusoidal signal while remaining within the boundaries of the three-dimensional workspace of the haptic device. Conversely, the mentee (another individual) is passively following the mentor's movements. Since haptic telementoring is a bilateral system, the data reduction distortion is in fact equally felt at the local and remote stations (assuming of course that the haptic data reduction parameters are set to equal values at both stations).

2) *Results*: The haptic data reduction technique is initially examined under a 6-DoF haptic telementoring setting. The average number of transmitted packets (percentage rate) with respect to the applied position and orientation deadband values are plotted in Fig. 2 (a). Also, the perceptibility

ratings of all 8 subjects and for the two experimental blocks were averaged as depicted in Fig. 2 (c). It can be observed from Fig. 2 (c) that for position and orientation deadbands that fall within the range [0.0 mm - 0.3 mm] and [0.0 rad - 0.003 rad] respectively, a perceptibility rating of at least 4 was obtained, which most participants described as fairly distortion-free. Moreover, with a perceptually tolerable position deadband of 0.3 mm and an orientation deadband of 0.003 rad, only 4.0% of the packets are transmitted. A closer investigation of the presented plots also revealed that with a small position deadband of 0.1 mm and an orientation deadband of 0.002 rad, only 6.9% of the packets are transmitted with a corresponding (and impressive) perceptibility rating of 4.9. Furthermore, when the data reduction technique is evaluated in a 3-DoF haptic telementoring setting with MPB Freedom 6S devices, (see Fig. 2 (b) and (d)), the amount of packets transmitted was reduced to 2.5% while still obtaining a perceptibility rating slightly over 4. It can also be seen that for a minuscule position deadband of 0.1 mm, only 4.3% of the packets are transmitted with a corresponding perceptibility rating of 4.9. In addition, it is interesting to observe that the haptic transmission and perceptibility rates obtained when using PHANTOM Desktop devices are considerably similar to the results attained when Freedom 6S devices are exploited. Furthermore, if a comparison is made between the data reduction results in Fig. 2 (a), (c) and those in Fig. 2 (b), (d), it can be observed that although the algorithm performs slightly better in 3-DoF settings, the results are still quite impressive when haptic devices with 6-DoFs are considered. Consequently, the algorithm scales well with the number of degrees of freedom.

VI. CONCLUSIONS

In this paper, a novel perception-based haptic data reduction technique has been presented to reduce network traffic in 6-DoF haptic-enabled telementoring systems. The experimental results demonstrated that the suggested method can achieve a considerable reduction of the packet rate without affecting the performance of the haptic telementoring system. To the best of the authors' knowledge, this is the first data reduction algorithm intended for 6-DoF telehaptic systems. Moreover, the proposed technique can in a straightforward manner be applied in similar teleoperation systems, such as in haptic telepresence and teleaction. Future work includes the evaluation of the proposed algorithm under more severe network conditions, including network-induced delay, jitter and packet loss.

REFERENCES

- [1] V. Nistor, B. Allen, G.P. Carman, P. Faloutsos, E. Dutson, "Haptic guided telementoring and videoconferencing system for laparoscopic surgery," SPIE International Symposium Smart Structures and Materials & Nondestructive Evaluation and Health Monitoring, March 2007.
- [2] S. Hirche, P. Hinterseer, E. Steinbach, Martin Buss, "Transparent data reduction in networked telepresence and teleaction systems. Part I: Communication without Time Delay," Presence: Teleoperators and Virtual Environments, vol. 16, no. 5, pp. 523-531, Oct. 2007.
- [3] S. Hirche, M. Buss, "Transparent data reduction in networked telepresence and teleaction systems. Part II: Time Delayed Communication," Presence: Teleoperators and Virtual Environments, vol. 16, no. 5, pp. 532-542, Oct. 2007.
- [4] P. Hinterseer, S. Hirche, S. Chaudhuri, E. Steinbach, M. Buss, "Perception-based data reduction and transmission of haptic data in telepresence and teleaction systems," IEEE Transactions on Signal Processing, vol. 56, no. 2, pp. 588-597, Feb. 2008.
- [5] R. M. Murray, Z. Li, and S. S. Sastry, "A Mathematical Introduction to Robotic Manipulation," CRC Press, Inc., 1994.
- [6] L. A. Jones, I. W. Hunter, "Human operator perception of mechanical variables and their effects on tracking performance," ASME Advances in Robotics, vol. 42, pp. 49-53, 1992.
- [7] G. C. Burdea, Force and touch feedback for virtual reality. New York: Wiley, 1996.
- [8] P. G. Otanez, J. R. Moyne, and D. M. Tilbury, "Using deadbands to reduce communication in networked control systems," American Control Conference, vol. 4, pp. 3015-3020, May 2002.
- [9] J. Kuffner, "Effective sampling and distance metrics for 3d rigid body path planning," IEEE International Conference on Robotics and Automation, vol. 4, pp. 3993-3998, May 2004.
- [10] F. Janabi-Sharif, V. Hayward, C. J. Chen, "Discrete-time adaptive windowing for velocity estimation," IEEE Transactions on Control Systems Technology, vol. 8, no. 6, pp. 1003-1009, Nov. 2000.
- [11] L. Rabiner, M. Sambur, C. Schmidt, "Applications of a nonlinear smoothing algorithm to speech processing," IEEE Transactions on Acoustics, Speech, and Signal Processing, vol. 23, no. 6, pp. 552-557, Dec. 1975.